P465L pparγ mutation confers partial resistance to the hypolipidemic action of fibrates.

Sergio Rodriguez-Cuenca[1]*, Stefania Carobbio[1,2]*, Gwendolyn Barceló-Coblijn[3], Xavier Prieur[4], Joana Relat[5,6], Ramon Amat[7], Mark Campbell[1], Ana Rita Dias[1], Myriam Bahri [1,2], Sarah L. Gray[8], and Antonio Vidal-Puig[1,2].

[1] University of Cambridge Metabolic. Research Laboratories, Level 4, Wellcome Trust-MRC Institute of Metabolic Science, Cambridge, UK.

[2] Wellcome Trust Sanger Institute, Wellcome Trust Genome Campus, Hinxton, Cambridge, UK.

[3] Institut d'Investigació Sanitària Illes Balears (IdISBa, Balearic Islands Health Research Institute), Palma, Balearic Islands, Spain.

[4] L'Institut du Thorax, INSERM, CNRS, Université de Nantes, Nantes, France.

[5] Department of Nutrition, Food Science and Gastronomy, School of Pharmacy and Food Science, Food and Nutrition Torribera Campus. University of Barcelona (UB), Santa Coloma de Gramenet (Spain); INSA-UB, Nutrition and Food Safety Research Institute, University of Barcelona, Barcelona, Spain..

[6] Institute of Biomedicine of the University of Barcelona (IBUB), Barcelona, Spain.

[7] Cell Signaling Unit, Departament de Ciències Experimentals i de la Salut, Universitat Pompeu Fabra (UPF), Barcelona, Spain.

[8] University of Northern British Columbia, Northern Medical Program, 3333 University Way, Prince George, BC, V2N 4Z9, Canada.

*These authors contributed equally to this work

CORRESPONDING AUTHORS EMAIL:

sr441@medschl.cam.ac.uk; sc547@medschl.cam.ac.uk; ajv22@medschl.cam.ac.uk

RUNNING TITLE: P465L pparγ mutation impairs pparα function.

Word count: 3397

Number of Figures: 5

Abstract:

Familial partial lipodystrophic syndrome 3 (FPLD3) is associated with mutations in the transcription factor PPARγ. The P467L mutant confers a dominant negative effect. We have previously investigated the pathophysiology of FPLD3 using a humanised mouse harbouring an equivalent mutation (P465L) in PPARγ that recapitulated the human clinical phenotype. One of the key clinical manifestations observed in humans and mice is the accumulation of fat in the liver. Here, we dissect the molecular mechanisms that facilitate accumulation of lipids in the liver and characterise the negative effect of the PPARγ mutation on the activation of PPARα *in vivo* by fibrates. P465L mice have increased insulin and FFAs, decreased secretion of VLDL when fed HFD and impaired hypolipidemic response to WY14643. Thus, the phenotype of PPARγ mutations may synergise with defects on PPARα function, indicating that the phenotype of the FPLD3 patients may not only be attributed to the dysfunction of PPARγ.

KEYWORDS: lipodystrophy, fatty liver, P465L ppar-gamma, ppar-alpha, fibrates.

Introduction:

Peroxisome proliferator-activated receptors (PPARs) regulate energy homeostasis and coordinate anabolic and catabolic biochemical processes. These transcription factors comprises three members: PPARγ (with two isoforms: PPARγ1 and PPARγ2), PPARα and PPARδ [1].

PPARγ regulates adipose tissue development and expansion, and harmonises lipogenic and lipolytic programmes [2]. Genetic defects in PPARγ [3] causes familial partial lipodystrophy syndrome type III (FPLD3) [4]. FPLD3 patients carrying the P467L mutation (rs121909244) exhibit lipodystrophic, hypertension, hepatic steatosis, hyperglycemia and severe dyslipidemia. This complex phenotype is recapitulated in the humanised P465L-PPARγ mutant mouse and exacerbated by specific nutritional challenges [5-7]. The PPARγ2 isoform is preferentially expressed in WAT and BAT. Other organs such as liver, predominantly express the PPARγ1 isoform but can induce the PPARγ2 isoform *de novo* under conditions of overnutrition [8]. This indicates that the repertoire of and relative amounts of PPARs coexisting in the same cell/tissue can differ according to specific nutritional status and metabolic requirements.

PPARα plays a fundamental role in lipid oxidation and biosynthesis, gluconeogenesis, cholesterol metabolism and ketogenesis [9]. PPARα is present in tissues with high rates of β-oxidation such as heart, skeletal muscle or liver [10]. Genetic ablation of PPARα in mice has revealed its involvement in fatty acid oxidation and the development of fatty liver and severe fasting hypoglycaemia when dysfunctional [11] [12]. Conversely, fibrates, a class of synthetic PPARα ligands, improve the manifestations of the metabolic syndrome in humans and rodents. For instance, the fibrate WY14643, decreases plasma triglycerides, reduces adiposity, and improves hepatic steatosis and insulin sensitivity in lipoatrophic mice [13].

PPARs share in common their co-activators, co-repressors and partners as well as their DNA responsive elements (PPRE). Thus, we hypothesised that changes in expression patterns and/or activity of PPARs may affect the transactivation capacity of the specific PPARs. At least in *in vitro*

studies, PPARs exhibit promiscuity in their binding to coactivators/corepressors and are involved in complex crosstalks. PPARα dominant negative mutants [14] or lacking ligand binding domain [15] exert cross-inhibition of the WT form of PPARα, and also of PPARγ and PPARδ, by competition for coactivators [14]. Moreover, the P467L PPARγ mutation also exerts a dominant negative effect on WT PPARγ *in vitro* [16] and by attenuating the release of corepressor and recruitment coactivators [17] it represses the activity of PPARα *in vitro* [14, 18]. The pathophysiological relevance *in vivo* of a crosstalk between PPARs has not been previously studied.

We have shown that the humanised P465L PPARγ murine model developed hepatic steatosis after four months on high fat diet (HFD) [5] recapitulating the phenotype of the P467L human [19]. Here, we dissect the mechanisms leading to this phenotype *in vivo* and provide evidence that the P465L PPARγ mutation promotes fatty liver through deficient transactivation PPARα. The P465L mice have fatty liver associated to hyperinsulinaemia, increased FFAs, decreased secretion of VLDL when fed HFD and impaired response to the hypolipidemic action of WY14643. The P465L PPARγ prevents the metabolic transcriptional activation and repression pattern mediated by PPARα and raises doubts that fibrates may be of use in the management of hypertriglyceridemia in FPLD3 patients carrying the dominant negative P467L mutation, in agreement with the clinical observation of recurrent hypertriglyceridemia despite fibrate treatment in FPLD3 patients [20-23].

Material and Methods:

Animals. P465L/+ PPARγ mice were generated as described previously [5]. Mice were fed standard chow or HFD (45%Kcal from fat) *ad libitum*, housed at 24C with 12h light cycle. Mice were separated into groups of 7-8 mice. Experimental groups of both genotypes included: chow diet/vehicle, chow diet/WY14643; HFD/vehicle and HFD/WY14643. Feeding of HFD started at the age of 5 weeks old for 28d. Then, mice were injected intraperitoneally vehicle or WY14643 (25mg/kg per day) for 5d. This research has been regulated under the Animals (Scientific

Procedures) Act 1986 Amendment Regulations 2012 following ethical review by the University of Cambridge, Animal Welfare and Ethical Review Body (AWERB).

Blood biochemistry. Enzymatic assay kits were used for plasma free fatty acids (Roche), tryglicerides, glucose and insulin according to manufacturer's instructions.

Liver triglycerides content. Hepatic lipid content was measured following Folch method as described [24].

Lipoprotein separation by FPLC. Lipoproteins from the pooled plasma of the experimental mice was isolated using FPLC according to the Diabetic Complications Consortium. https://www.diacomp.org/shared/document.aspx?id=14&docType=Protocol.

Glycogen determination. Hepatic glycogen content was measured as previously described [25].

Histology. The livers were dissected and fixed in 10% formalin, cryoprotected (20% sucrose) and frozen in chilled isopentane prior to sectioned using a cryostat and stained for lipid with Oil Red O.

Lipid analysis. Liver tissue was homogenized with a tissue blender. Lipids were extracted using n-hexane/2-propanol. Tissue extracts were centrifuged at 1,000g to pellet debris. The lipid-containing organic phase was stored under nitrogen at −80°C [26, 27]. Total lipids were subjected to transesterification, converting the acyl chains to fatty acid methyl esters (FAME) [28]. Heptadecanoic acid (17:0) was the internal standard. Individual FAMEs were separated by gas liquid chromatography using a SP-2330 column (0.32 mm ID, 30 m length) and a gas chromatograph equipped with dual autosamplers and dual flame ionization detectors.

Retrotranscription and Real-Time PCR analysis. Total RNA was isolated from the liver with Trizol. 1000ng of the total RNA was RT to cDNA and Real-time PCR was performed as previously described [5]. Expression of target genes was corrected by the geometrical average of four different housekeeping genes: 18S, β2-microglobulin, β-actin and 36B4.

Statistical analysis. 3-way ANOVA was used for the analysis of the interaction between genotype (G), diet (D) and treatment (T) or fasting (F). SPSS14 was used as statistical software.

Results

P465L PPARγ mutant mice are hyperlipidemic and hyperinsulinemic.

P465L mutant mice had higher levels of FFAs, TGs and cholesterol in serum than WT mice (Fig1a), independently of the diet, recapitulating the hyperlipidemia observed in the P467L human carriers. On chow diet and after a short challenge with HFD, P465L mice were normoglycemic despite hyperinsulinemia suggesting insulin secretion compensated for peripheral insulin resistance; nevertheless, when challenged with HFD for 3months, P465L mice became hyperglycemic (SFig1). P465L mice also had increased hepatic glycogen levels in the fed state (SFig2a).

P465L PPARγ mutant mice are resistant to the hypolipidemic action of WY14643.

Treatment with WY14643 reduced plasma TGs in WT mice, but failed to do so in P465L mice suggesting resistance against the hypolipidemic action of fibrates. By contrast, WY14643 increased plasma cholesterol levels in both genotypes as previously reported [29] and also increased 3-hydroxybutyrate in both genotypes. The increase in 3-hydroxybutyrate (Fig1) is compatible with fibrate induction of hepatic β-oxidation, an effect that was more robust in the P465L mice, particularly when fed HFD. Interestingly, when fasted o/n, the P465L mice had significantly higher levels of 3-hydroxybutyrate than WT mice (SFig1), reflecting the increased hepatic FFA delivery and β-oxidation in P465L livers. At the organismal level, the acute treatment with WY14643 induced hepatomegaly in both genotypes, and a specific decrease in the fat mass of WT mice but not in P465L mice on HFD (Fig1b). This suggested that the P465L mutation conferred resistance to the pro-lipolytic effect of fibrates in adipose tissue [30]. All these *in vivo* data supported that PPARγ P465L mutation conferred partial resistance to the action of fibrates both liver and adipose tissue.

P465L PPARγ mutation promotes fatty liver and alterations in lipoprotein metabolism.

We have shown before that P465L mice increased liver mass and hepatic TG content when fed HFD for 16w or when backcrossed with the ob/ob mouse [5]. Now, we show that in mice fed HFD (45%Kcal) for 4w, levels of hepatic TGs in P465L are already marginally higher than WT

mice. However, an unexpected finding was that HFD together with fibrate treatment increased hepatic fat in P465L but not in WT mice (Fig2a). Moreover, P465L mice exhibited more hepatic fat after o/n fasting than WT counterparts, further supporting that the fat accumulated within liver cells predominantly originated from adipose tissue (transient steatosis) (SFig1). Overall, these data further reinforced the hypothesis of a PPARα contribution (e.g. fibrates/fasting) regulating storage, oxidation and/or release of hepatic lipids in P465L mice.

P465L PPARγ increases hepatic MUFA/PUFA ratio.

The analysis of hepatic fatty acid composition (Fig2b) showed that on a HFD, the P465L mice had increased levels of MUFA in liver associated with increased SCD1 index reflecting the active conversion of saturated (SFA) into monounsaturated fatty acids (MUFA), the preferred substrate for triglyceride storage. Despite the increase in the SCD1 index, *scd1* and *scd2* mRNAs were downregulated revealing a mismatch between enzymatic flux and gene regulation. Low PUFA content in HFD fed P465L livers was accounted for by reduced levels of 20:5n3, 22:5n3, 22:6n3 and 20:3n6 and 20:4n6 but not of 18:2n6 whose levels were increased in P465L, indicating impaired biosynthesis of PUFAs. Gene expression did not reveal changes in the expression of elongases and desaturases (Fig2c); however, the FADS1 index (20:4n6/20:3n6) was downregulated in P465L livers. Interestingly, FADS2 activity [(20:3n-6)/(18:2n-6) ratio] was increased in WT mice treated with WY14643 but less in P465L mice (SFig2b). Also, the expression of *fads3* [31], was downregulated in P465L livers, suggesting *fads3* may be a new desaturase transcriptionally regulated by PPARγ.

P465L PPARγ impairs VLDL secretion in HFD fed mice.

We investigated whether changes in the lipoprotein lipid composition in P465L mice mirrored their increased fat accumulation in liver and blunted functional effect of fibrates (Fig3ab). The hypolipidaemic effects of fibrates involve enhanced catabolism of TG rich particles (increase LPL and decrease apoCIII) and decreased in ApoB and VLDL production. In chow fed conditions plasma levels of VLDL-TG in P465L mice were larger than in WT. *A priori*, increased levels of

VLDL in P465L mice may be related to hyperinsulinemia, increased hepatic influx of FFA, hepatic accumulation of TG and increased VLDL-TG secretion. However, what was unexpected was that on HFD, the P465L mice showed a paradoxical decrease in VLDL-TG levels compared to WT controls. Moreover, WY14643 did not change VLDL-TG levels in chow fed mice of any genotype, and only slightly decreased VLDL-TG in WT mice fed HFD in line with the effects of fibrates in VLDL secretion. As previously mentioned, on HFD the–P465L mice showed a paradoxical reduction in the plasma VLDL-TG levels, despite high fatty acid levels. Of potential mechanistic relevance, P465L livers had increased expression of lipid droplet proteins such as *adrp/plin2*, *fsp27/cidec* and *s3-12/plin4* as well as the fatty acid binding protein *fabp4/ap2* (Fig3c).

Gene expression analysis confirmed that mRNAs of hepatic (Fig3b) and adipose LPL (SFig3a), and *cd36* and *fatp1* fatty acid transporters in skeletal muscle (SFig3b) were decreased in P465L mice, thus likely contributing to the impaired peripheral metabolism of VLDL-TG in P465L mutants. Of note, *apoIV* gene expression, previously associated to hepatic steatosis and secretion of large TG-enriched apoB-containing VLDL [32], was increased in P465L livers, independently of the nutritional and pharmacological treatment. We also observed a genotype dependent decrease in the levels of *apob* and minor differences in *mttp*.

We analysed the effect of P465L on HDL lipoproteins. Unlike in humans where fibrates increase HDL-C levels and *apoa1* expression [33], fibrates do not decrease HDL nor *apoa1* expression in wildtype non transgenic mice [34, 35]. Surprisingly, in the P465L mice, fed chow or HFD, fibrates increased HDL levels in comparison to WT mice indicating that P465L pparγ mutation interferes (directly or indirectly) with the expected response to fibrates on HDL metabolism. We also observed an increased *apoa2/apoa1* mRNA ratio in P465L mice (Fig3b). Increased levels of *apoa2* have been associated with increased pro-oxidative and pro-inflammatory responses, alterations in HDL metabolization and increased atherogenic risk [36]. Altogether, the changes observed in P465L mutants suggest a deleterious effect on HDL metabolism.

WY14643 increased cholesterol enriched IDL/LDL-C levels in both genotypes. A similar effect has been observed in fenofibrate-treated mice fed high fat/high sucrose diets [37] and also in patients with severe dyslipidaemia [38]. We observed that on a HFD, treatment with WY14643 reduces triglyceride enriched IDL/LDL-TG in WT but not in P465L mice (Fig2B). This is in agreement with the metabolisation of TGs from the IDL/LDL fraction, and likely mediated by hepatic or peripheral lipases in WT mice vs. P465L mice (where both levels of HL and LDLR are reduced).

Hepatic mitochondrial and peroxisomal FAO genes are downregulated in HFD fed P465L mice.

Fibrates promote a metabolic switch towards the use of fatty acid as energetic substrates. Fibrates activate the pyruvate dehydrogenase kinases PDK2 and PDK4, which inactivate pyruvate dehydrogenase and enhance the utilization of serum fatty acids and triglycerides [39]. P465L livers showed reduced hepatic expression of *pdk4* and a blunted increase response to WY14643 in comparison to WT (Fig4a). Thus, the P465L mutation conferred resistance to the induction of fatty acid oxidation (FAO) by WY14643. We hypothesised that PPARγ P465L may induce dysfunction of the mitochondrial and/or peroxisomal FAO programmes that could contribute to the development of fatty liver and liver damage [40, 41] in P465L mice.

P465L mutant mice showed reduced expression of mFAO and pFAO genes in chow fed vs. WT counterparts (Fig4b). These data may be interpreted as either P465L PPARγ preventing basal expression of genes regulated by PPARα, and/or that physiological expression PPARγ itself may impair the expression of these genes.

There is substantial literature showing a pro-oxidative role for PPARα [42, 43] and in line with this, the fibrate WY14643 increased the expression of most of the genes associated to mFAO and pFAO programmes in both genotypes. However, a set of genes from both programmes failed to be upregulated in P465L livers in response to WY14643. Specifically *abcd1, phyh, idh, ech1, decr2,* failed to be induced by fibrates in P465L liver, indicative of the selective resistance to fibrates. We

also identified genes that responded differently in P465L vs WT liver, in response to different diets (*lcad, mcad, vlcas, amarc, mylcd*) suggesting an interaction effect of the genotype with fibrates and dietary challenges.

P465L PPARγ interferes with the transrepression capacity of PPARα.

Fibrates exert anti-fibrotic and anti-inflammatory effects through transrepressive mechanisms [44]. We observed that in HFD fed WT mice, administration of WY14643 reduces the expression of target genes such as *saa1* and *saa2* and *fibrinogen* (Fig5). Interestingly, this effect was not observed in P465L mice indicating defective transrepression activity of PPARα.

Discussion

This work follows our previous research showing that the P465L mouse recapitulates the phenotype of FPLD3 patients and is characterised by a severe partial lipodystrophic phenotype associated with insulin resistance, fatty liver, hypertension and increased atherosclerotic lesions. Here, we provide *in vivo* evidence that the development of the fatty liver observed in the P465L PPARγ knock-in mouse involves impairment in the transcriptional activity of PPARα. This is supported by *in vivo* data showing that P465L mice develops fatty liver on a HFD and are resistant to WY14643, a fibrate that acts as a PPARα activator. This phenotype is highly reminiscent of the resistance to fibrates observed in PPARα KO mice. In response to WY14643, the size of the fat depots decreases in WT mice in contrast with the adipose tissue of the P465L that remain unaffected. Similarly, WY14643 treated WT mice showed a reduction in hepatic TG content, whereas P465L remains insensitive to fibrate effect when fed HFD. Additionally, we observed the unexpected increase in hepatic TG during the fed/fasting transition in P465L mice with both, chow and HFD feeding. These responses are consistent with partial resistance to the effects of PPARα activation in P465L mice *in vivo*.

Our data also shows that the PPARγ P465L mutant interferes with the lipoprotein profile and its regulation by fibrates. We observed an interesting shift in the lipoprotein fingerprint between chow and HFD fed P465L mice. On a chow diet, P465L mice had increased levels of VLDL, which is consistent with the expected increased flux of fatty acids resulting from PPARγ induced adipose tissue dysfunction and hyperinsulinemia. However, when fed HFD for one month, this pattern was reversed, showing a paradoxical decrease of VLDL which was associated with increased expression of hepatic lipid droplet proteins in the P465L PPARγ mutant livers. Whether this increase in lipid droplet protein expression is directly mediated by a defect on the transcriptional programme of PPARγ or a secondary perturbation is unclear. However, it is known that PPARγ and PPARα are both transcriptional regulators of *adrp* and *fsp27* [45] and that the overexpression of *fsp27 and adrp/plin2* prevent the access of lipases to the core of the lipid droplet thus impairing the hydrolysis of TG [46, 47]. Thus, the observed increased expression of lipid droplet proteins [48] contribute to the trapping and accumulation of lipids in the in P465L mice leading to hepatic steatosis. Of note, in P465L livers, *fsp27* expression is further increased by fibrates; which may contribute to the increase in the hepatic TG levels observed when fed HFD and treated with fibrates. The apparent paradox of PPARα simultaneously promoting storage through the expression of lipid droplet proteins and oxidation, suggests a role for PPARα activating transcriptional programmes aimed at reducing the accumulation of toxic lipid species by diverting them either to a safe storage and/or metabolising them. This apparently opposed functions may explain some controversial results regarding the use of fibrates against fatty liver in rodent models [49, 50].

The general assumption is that the association between lipodystrophy and NAFLD is consequence of the failure of the adipose tissue to expand resulting in spillage of lipids into the liver. Here, we provide evidence that the fatty liver of the P465L lipodystrophic mice also exhibit qualitative changes (increased MUFA/PUFA ratio) in its lipid composition. These data are consistent with the characteristic changes in lipid biosynthetic pathways observed in "classical

models" of NAFLD. This indicates that the qualitative changes in the fatty acid composition observed in P465L livers may not be specific but a common pathogenic feature of mechanisms operating in NAFLD.

The expression profiling revealed impairment of PPARα preferentially regulated genes in P465L mice on a chow diet. This suggests that even when PPARα ligands are present at low physiological levels, the presence of the P465L mutation is enough to dysregulate the expression of those genes at a transcriptional level. This includes mitochondrial and peroxisomal FAO genes, well-known targets of PPARα. The P465L mice fed a chow diet showed impaired expression of genes controlling mFAO and pFAO, and these effects were partially masked after treatment with WY14643 and/or HFD. Additionally, in P465L livers we also identified PPARa target genes that were unresponsive to treatment with fibrates further supporting the concept of resistance to ligand-dependent activation of PPARα by P465L PPARγ. Interestingly, these genotype mediated differences were not observed in the fasted state, indicating that the effect of the P465L mutation on PPARα function is more pathophysiologically relevant when the expression/activity of PPARα is below a particular threshold, when PPARγ is more active or when it is overcome by the hormonal adaptation taking place in response to starvation.

Despite the fact that our experimental model was not designed to induce severe liver damage, we found that the expression of some genes involved in fibrosis, known to be downregulated by PPARα, were induced in P465L livers, suggesting that transrepression activity of PPARα was also impaired by the presence of the P465L PPARγ mutant.

Globally considered, these data indicate that the fatty liver observed in P465L mice may result from alterations at local level involving uncoupling of lipid storage in lipid droplets from VLDL assembly and secretion, an impaired hepatic FAO in a context where defective adipose tissue and inefficient peripheral uptake of lipids are likely to be decreased.

In summary, we have shown that P465L mice develop hepatic steatosis associated to impaired VLDL secretion/increased lipid trapping in liver, as well as qualitative changes in the hepatic fatty acid repertoire characteristic of common NAFLD models. We also provide biochemical data, hepatic lipid content and evidence of impaired expression of a number of well-established PPARα target genes in P465L livers to conclude that similarly to *in vitro* data, P465L confers partial resistance against the hypolipidemic action of fibrates *in vivo*. The fatty liver phenotype observed in P465L mutant mice is not only consequence of dysfunctional adipose tissue, but also related to hepatic defective lipid metabolism. Our results questions the potential value of fibrates for the management of hypertriglyceridemia/NAFLD in FPLD3, particularly of those patients carrying the PPARγ-P467L mutation. At more global level, our data indicate the importance of the precise repertoire of PPARs present under specific metabolic conditions, to define the best therapeutic strategy and modulate the fine balance between metabolically opposed functions.

Funding

This work was funded by Wellcome Trust, MRC MDU (MC_UU_12012/2), FP7-MITIN (Integration of the System Models of Mitochondrial Function and Insulin Signalling and its Application in the Study of Complex Diseases (Grant Agreement 223450) and H2020 EPoS Elucidating Pathways of Steatohepatitis. (Grant Agreement 634413). Disease Model Core, Biochemistry Assay Lab and the Histology Core are funded by [MRC_MC_UU_12012/5] and Wellcome Trust Strategic Award [100574/Z/12/Z].

Author Contributions. SRC and SC conceived the original hypothesis, designed and performed experiments in vivo/ex vivo and wrote the manuscript. GBC performed the fatty acid composition analysis, discussed and edited the manuscript. XP performed the lipoprotein profiling, discussed and edited the manuscript, RA, JR, MC, RD and MB contributed to ex vivo profiling, discussed and edited the manuscript. SG conceived the original hypothesis, designed experiments and wrote the manuscript. AVP conceived the original hypothesis, designed experiments and wrote the manuscript. AVP is the guarantor of this work. All authors approved its publication.

Conflict of interest. The authors declare that they have no conflict of interest.

FIGURE LEGENDS

FIGURE1. (a) Blood biochemistry and Body composition (b) from P465L pparγ mutant mice vs. WT mice fed chow or HFD, with or without WY14643 (ip:25mg/kg). Graphs represent the average of 7-8 mice per group ± SEM analysed by ANOVA ($p<0.05$). Different colour circles denote genotype effect (blue), treatment (red), diet (green), interactive effect genotype x treatment (black), genotype x diet (white), diet x treatment (grey) and genotype x treatment x diet (orange).

FIGURE2. (a) Oil Red O -stained sections (10×) and triglyceride composition of liver from P465L pparγ mutant mice vs. WT mice fed chow or HFD, with or without WY14643 (ip:25mg/kg). Graphs represent the average of 7-8 mice per group ± SEM. (b) Fatty acid composition in molar percentage of hepatic fatty acids from P465L pparγ mutant mice vs. WT mice fed chow or HFD, with or without WY14643 (ip:25mg/kg). (c) Hepatic gene expression of candidate genes relevant in *de novo* lipogenesis and PUFA biosynthesis and analysed by ANOVA ($p<0.05$). Different colour circles denote Genotype effect (blue), treatment (red), diet (green), interactive effect genotype x treatment (black), genotype x diet (white), diet x treatment (grey) and genotype x treatment x diet (orange).

FIGURE3. (a) Lipoprotein cholesterol and TG distribution were determined in plasma from non-fasted P465L pparγ mutant mice vs. WT mice fed chow or HFD, with or without WY14643 (ip:25mg/kg). Approximate elution volumes for particles in the size ranges of VLDL, LDL, and HDL are indicated (b) Hepatic gene expression of candidate genes relevant in lipoprotein metabolism and (c) lipid droplet proteins is shown as log2 conversions of average gene expression data relative to controls (log2 100 = 6.6). Magnitude > 6.6 and < 6.6 denotes up- and downregulation, respectively, compared with WT, chow fed controls and analysed by ANOVA ($p<0.05$). Different colour circles denote Genotype effect (blue), treatment (red), diet (green), interactive effect genotype x treatment (black), genotype x diet (white), diet x treatment (grey) and genotype x treatment x diet (orange).

FIGURE4. (a) Hepatic gene expression of candidate genes relevant in (a) glucose metabolism (b) fatty acid uptake and mitochondrial/peroxisomal fatty acid oxidation programmes and (c) nuclear transcription factors is shown as log2 conversions of average gene expression data relative to controls (log2 100 = 6.6). Magnitude > 6.6 and < 6.6 denotes up- and downregulation, respectively, compared with WT, chow fed controls and analysed by ANOVA ($p<0.05$). Different colour circles denote Genotype effect (blue), treatment (red), diet (green), interactive effect genotype x treatment (black), genotype x diet (white), diet x treatment (grey) and genotype x treatment x diet (orange).

FIGURE5. (a) Hepatic gene expression of candidate genes relevant in inflammation and fibrosis is shown as log2 conversions of average gene expression data relative to controls (log2 100 = 6.6). Magnitude > 6.6 and < 6.6 denotes up- and downregulation, respectively, compared with WT, chow fed controls and analysed by ANOVA ($p<0.05$). Different colour circles denote Genotype effect (blue), treatment (red), diet (green), interactive effect genotype x treatment (black), genotype x diet (white), diet x treatment (grey) and genotype x treatment x diet (orange).

REFERENCES

[1] Evans RM, Barish GD, Wang YX. PPARs and the complex journey to obesity. Nat Med. 2004; **10**: 355-361

[2] Rodriguez-Cuenca S, Carobbio S, Velagapudi VR, *et al.* Peroxisome proliferator-activated receptor gamma-dependent regulation of lipolytic nodes and metabolic flexibility. Mol Cell Biol. 2012; **32**: 1555-1565

[3] Majithia AR, Tsuda B, Agostini M, *et al.* Prospective functional classification of all possible missense variants in PPARG. Nat Genet. 2016; **48**: 1570-1575

[4] Garg A. Acquired and inherited lipodystrophies. N Engl J Med. 2004; **350**: 1220-1234

[5] Gray SL, Nora ED, Grosse J, *et al.* Leptin deficiency unmasks the deleterious effects of impaired peroxisome proliferator-activated receptor gamma function (P465L PPARgamma) in mice. Diabetes. 2006; **55**: 2669-2677

[6] Kis A, Murdoch C, Zhang M, *et al.* Defective peroxisomal proliferators activated receptor gamma activity due to dominant-negative mutation synergizes with hypertension to accelerate cardiac fibrosis in mice. Eur J Heart Fail. 2009; **11**: 533-541

[7] Pendse AA, Johnson LA, Tsai YS, Maeda N. Pparg-P465L mutation worsens hyperglycemia in Ins2-Akita female mice via adipose-specific insulin resistance and storage dysfunction. Diabetes. 2010; **59**: 2890-2897

[8] Vidal-Puig A, Jimenez-Linan M, Lowell BB, *et al.* Regulation of PPAR gamma gene expression by nutrition and obesity in rodents. J Clin Invest. 1996; **97**: 2553-2561

[9] Oosterveer MH, Grefhorst A, van Dijk TH, *et al.* Fenofibrate simultaneously induces hepatic fatty acid oxidation, synthesis, and elongation in mice. J Biol Chem. 2009; **284**: 34036-34044

[10] Issemann I, Green S. Activation of a member of the steroid hormone receptor superfamily by peroxisome proliferators. Nature. 1990; **347**: 645-650

[11] Hashimoto T, Cook WS, Qi C, Yeldandi AV, Reddy JK, Rao MS. Defect in peroxisome proliferator-activated receptor alpha-inducible fatty acid oxidation determines the severity of hepatic steatosis in response to fasting. J Biol Chem. 2000; **275**: 28918-28928

[12] Guerre-Millo M, Rouault C, Poulain P, *et al.* PPAR-alpha-null mice are protected from high-fat diet-induced insulin resistance. Diabetes. 2001; **50**: 2809-2814

[13] Chou CJ, Haluzik M, Gregory C, *et al.* WY14,643, a peroxisome proliferator-activated receptor alpha (PPARalpha) agonist, improves hepatic and muscle steatosis and reverses insulin resistance in lipoatrophic A-ZIP/F-1 mice. J Biol Chem. 2002; **277**: 24484-24489

[14] Semple RK, Meirhaeghe A, Vidal-Puig AJ, *et al.* A dominant negative human peroxisome proliferator-activated receptor (PPAR){alpha} is a constitutive transcriptional corepressor and inhibits signaling through all PPAR isoforms. Endocrinology. 2005; **146**: 1871-1882

[15] Gervois P, Torra IP, Chinetti G, *et al.* A truncated human peroxisome proliferator-activated receptor alpha splice variant with dominant negative activity. Mol Endocrinol. 1999; **13**: 1535-1549

[16] Barroso I, Gurnell M, Crowley VE, *et al.* Dominant negative mutations in human PPARgamma associated with severe insulin resistance, diabetes mellitus and hypertension. Nature. 1999; **402**: 880-883

[17] Leff T, Mathews ST, Camp HS. Review: peroxisome proliferator-activated receptor-gamma and its role in the development and treatment of diabetes. Exp Diabesity Res. 2004; **5**: 99-109

[18] Savage DB, Tan GD, Acerini CL, *et al.* Human metabolic syndrome resulting from dominant-negative mutations in the nuclear receptor peroxisome proliferator-activated receptor-gamma. Diabetes. 2003; **52**: 910-917

[19] Hegele RA. Lessons from human mutations in PPARgamma. Int J Obes (Lond). 2005; **29 Suppl 1**: S31-35
[20] Francis GA, Li G, Casey R, *et al.* Peroxisomal proliferator activated receptor-gamma deficiency in a Canadian kindred with familial partial lipodystrophy type 3 (FPLD3). BMC Med Genet. 2006; **7**: 3
[21] Guettier JM, Park JY, Cochran EK, *et al.* Leptin therapy for partial lipodystrophy linked to a PPAR-gamma mutation. Clin Endocrinol (Oxf). 2008; **68**: 547-554
[22] Monajemi H, Zhang L, Li G, *et al.* Familial partial lipodystrophy phenotype resulting from a single-base mutation in deoxyribonucleic acid-binding domain of peroxisome proliferator-activated receptor-gamma. J Clin Endocrinol Metab. 2007; **92**: 1606-1612
[23] Sleilati GG, Leff T, Bonnett JW, Hegele RA. Efficacy and safety of pioglitazone in treatment of a patient with an atypical partial lipodystrophy syndrome. Endocr Pract. 2007; **13**: 656-661
[24] Folch J, Lees M, Sloane Stanley GH. A simple method for the isolation and purification of total lipides from animal tissues. J Biol Chem. 1957; **226**: 497-509
[25] Pons A, Roca P, Aguilo C, Garcia FJ, Alemany M, Palou A. A method for the simultaneous determination of total carbohydrate and glycerol in biological samples with the anthrone reagent. J Biochem Biophys Methods. 1981; **4**: 227-231
[26] Castagnet PI, Golovko MY, Barcelo-Coblijn GC, Nussbaum RL, Murphy EJ. Fatty acid incorporation is decreased in astrocytes cultured from alpha-synuclein gene-ablated mice. J Neurochem. 2005; **94**: 839-849
[27] Hara A, Radin NS. Lipid extraction of tissues with a low-toxicity solvent. Anal Biochem. 1978; **90**: 420-426
[28] Brockerhoff H. Determination of the positional distribution of fatty acids in glycerolipids. Methods Enzymol. 1975; **35**: 315-325
[29] Lu Y, Boekschoten MV, Wopereis S, Muller M, Kersten S. Comparative transcriptomic and metabolomic analysis of fenofibrate and fish oil treatments in mice. Physiol Genomics. 2011; **43**: 1307-1318
[30] Ferreira AV, Parreira GG, Green A, Botion LM. Effects of fenofibrate on lipid metabolism in adipose tissue of rats. Metabolism. 2006; **55**: 731-735
[31] Blanchard H, Legrand P, Pedrono F. Fatty Acid Desaturase 3 (Fads3) is a singular member of the Fads cluster. Biochimie. 2011; **93**: 87-90
[32] VerHague MA, Cheng D, Weinberg RB, Shelness GS. Apolipoprotein A-IV expression in mouse liver enhances triglyceride secretion and reduces hepatic lipid content by promoting very low density lipoprotein particle expansion. Arterioscler Thromb Vasc Biol. 2013; **33**: 2501-2508
[33] Tsunoda F, Asztalos IB, Horvath KV, Steiner G, Schaefer EJ, Asztalos BF. Fenofibrate, HDL, and cardiovascular disease in Type-2 diabetes: The DAIS trial. Atherosclerosis. 2016; **247**: 35-39
[34] Berthou L, Duverger N, Emmanuel F, *et al.* Opposite regulation of human versus mouse apolipoprotein A-I by fibrates in human apolipoprotein A-I transgenic mice. J Clin Invest. 1996; **97**: 2408-2416
[35] Vu-Dac N, Chopin-Delannoy S, Gervois P, *et al.* The nuclear receptors peroxisome proliferator-activated receptor alpha and Rev-erbalpha mediate the species-specific regulation of apolipoprotein A-I expression by fibrates. J Biol Chem. 1998; **273**: 25713-25720
[36] Castellani LW, Lusis AJ. ApoA-II versus ApoA-I: two for one is not always a good deal. Arterioscler Thromb Vasc Biol. 2001; **21**: 1870-1872
[37] Fernandes-Santos C, Carneiro RE, de Souza Mendonca L, Aguila MB, Mandarim-de-Lacerda CA. Pan-PPAR agonist beneficial effects in overweight mice fed a high-fat high-sucrose diet. Nutrition. 2009; **25**: 818-827

[38] Davignon J, Roederer G, Montigny M, *et al.* Comparative efficacy and safety of pravastatin, nicotinic acid and the two combined in patients with hypercholesterolemia. Am J Cardiol. 1994; **73**: 339-345
[39] Motojima K. A metabolic switching hypothesis for the first step in the hypolipidemic effects of fibrates. Biol Pharm Bull. 2002; **25**: 1509-1511
[40] Cherkaoui-Malki M, Surapureddi S, El-Hajj HI, Vamecq J, Andreoletti P. Hepatic steatosis and peroxisomal fatty acid beta-oxidation. Curr Drug Metab. 2012; **13**: 1412-1421
[41] Mantena SK, King AL, Andringa KK, Eccleston HB, Bailey SM. Mitochondrial dysfunction and oxidative stress in the pathogenesis of alcohol- and obesity-induced fatty liver diseases. Free Radic Biol Med. 2008; **44**: 1259-1272
[42] Chamouton J, Latruffe N. PPARalpha/HNF4alpha interplay on diversified responsive elements. Relevance in the regulation of liver peroxisomal fatty acid catabolism. Curr Drug Metab. 2012; **13**: 1436-1453
[43] Rodriguez C, Cabrero A, Roglans N, *et al.* Differential induction of stearoyl-CoA desaturase and acyl-CoA oxidase genes by fibrates in HepG2 cells. Biochem Pharmacol. 2001; **61**: 357-364
[44] Pawlak M, Bauge E, Bourguet W, *et al.* The transrepressive activity of peroxisome proliferator-activated receptor alpha is necessary and sufficient to prevent liver fibrosis in mice. Hepatology. 2014; **60**: 1593-1606
[45] de la Rosa Rodriguez MA, Kersten S. Regulation of lipid droplet-associated proteins by peroxisome proliferator-activated receptors. Biochim Biophys Acta. 2017; **1862**: 1212-1220
[46] Langhi C, Baldan A. CIDEC/FSP27 is regulated by peroxisome proliferator-activated receptor alpha and plays a critical role in fasting- and diet-induced hepatosteatosis. Hepatology. 2015; **61**: 1227-1238
[47] Rajamoorthi A, Arias N, Basta J, Lee RG, Baldan A. Amelioration of diet-induced steatohepatitis in mice following combined therapy with ASO-Fsp27 and fenofibrate. J Lipid Res. 2017:
[48] Fujii H, Ikura Y, Arimoto J, *et al.* Expression of perilipin and adipophilin in nonalcoholic fatty liver disease; relevance to oxidative injury and hepatocyte ballooning. J Atheroscler Thromb. 2009; **16**: 893-901
[49] Edvardsson U, Ljungberg A, Linden D, *et al.* PPARalpha activation increases triglyceride mass and adipose differentiation-related protein in hepatocytes. J Lipid Res. 2006; **47**: 329-340
[50] Shiri-Sverdlov R, Wouters K, van Gorp PJ, *et al.* Early diet-induced non-alcoholic steatohepatitis in APOE2 knock-in mice and its prevention by fibrates. J Hepatol. 2006; **44**: 732-741

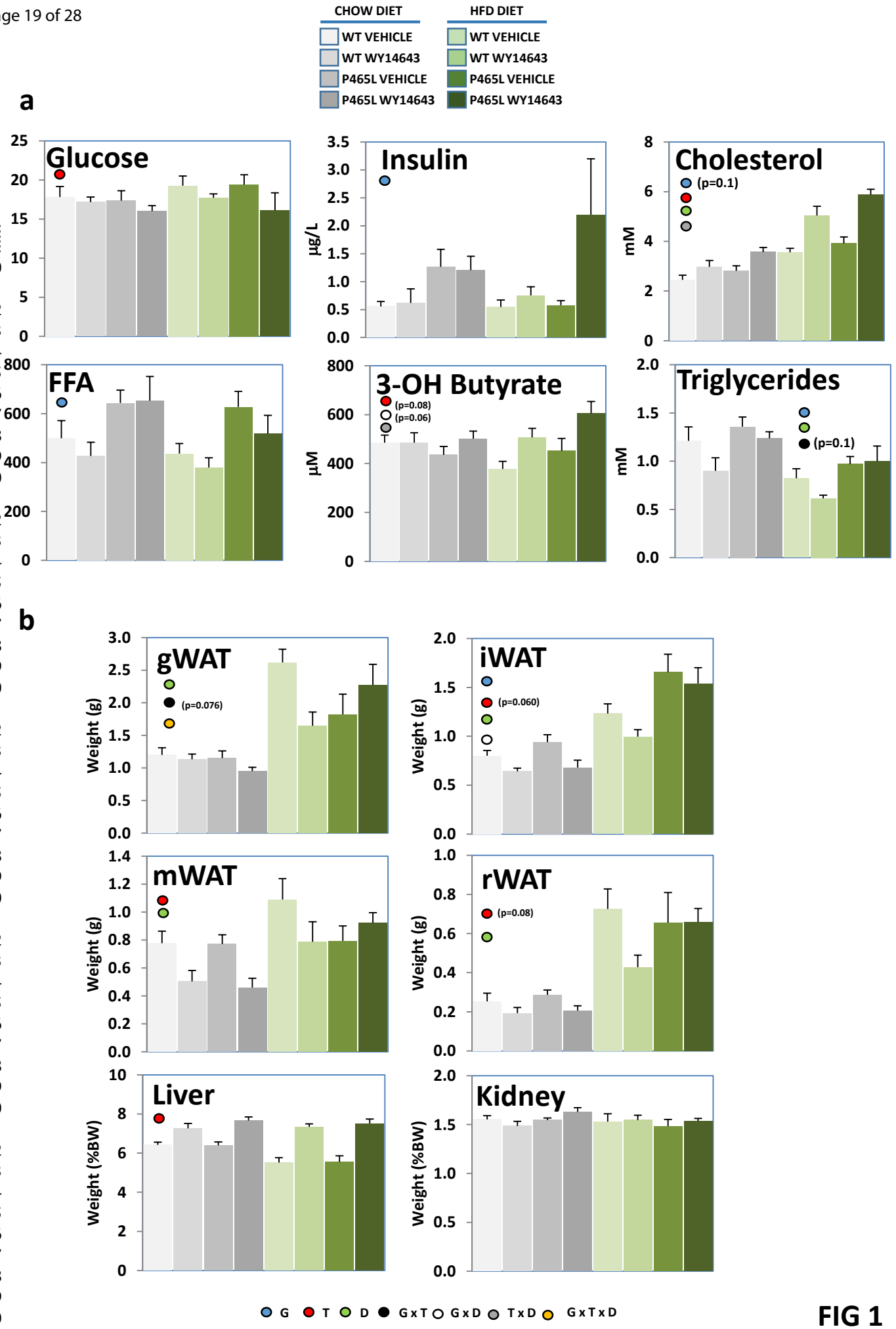
CHOW DIET
WT VEHICLE
WT WY14643
P465L VEHICLE
P465L WY14643
HFD DIET
WT VEHICLE
WT WY14643
P465L VEHICLE
P465L WY14643
a
Glucose
mM
Insulin
µg/L
Cholesterol
(p=0.1)
mM
FFA
µM
3-OH Butyrate
(p=0.08)
(p=0.06)
µM
Triglycerides
(p=0.1)
mM
b
gWAT
(p=0.076)
Weight (g)
iWAT
(p=0.060)
Weight (g)
mWAT
Weight (g)
rWAT
(p=0.08)
Weight (g)
Liver
Weight (%BW)
Kidney
Weight (%BW)
G
T
D
GxT
GxD
TxD
GxTxD

FIG 1

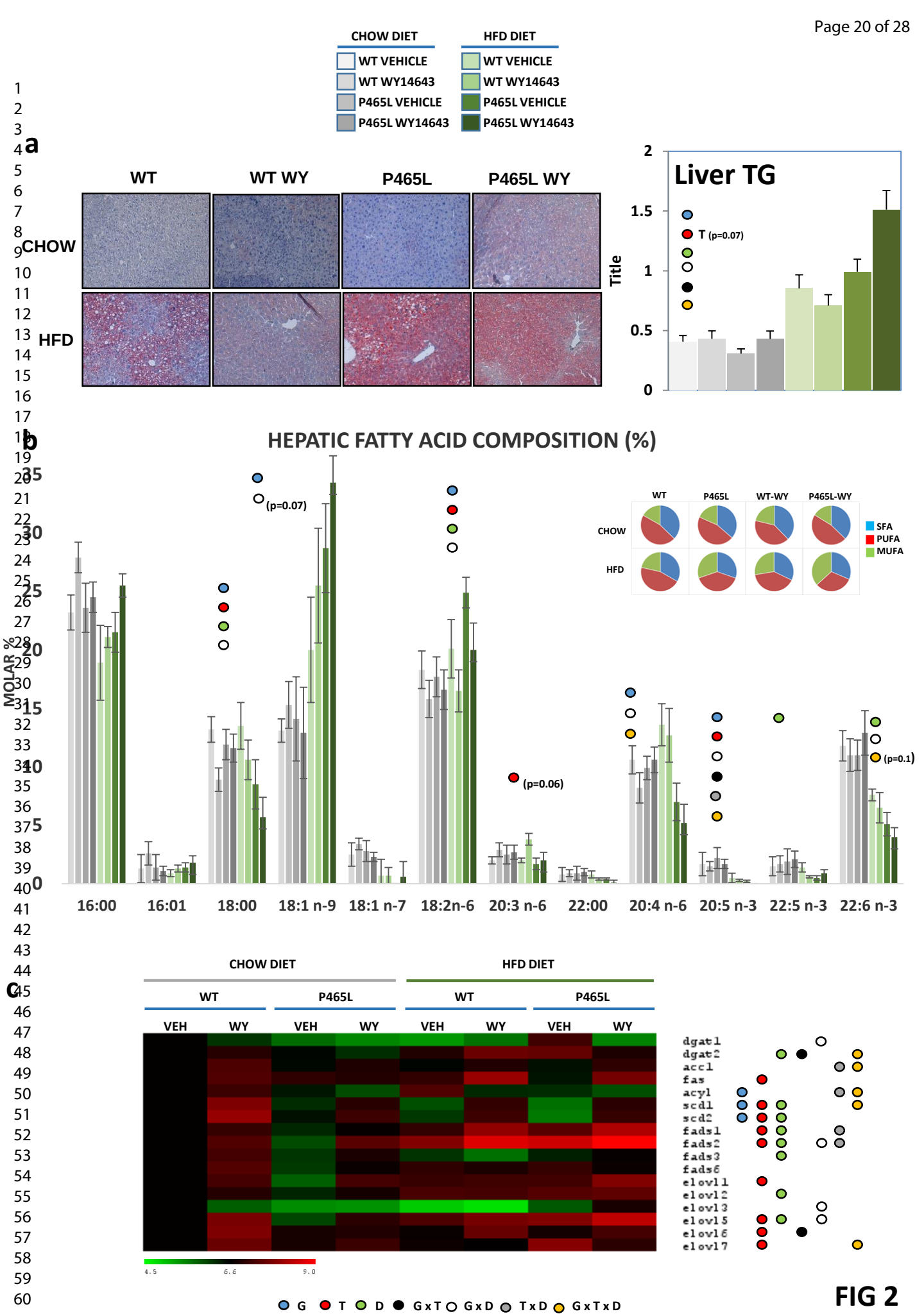
CHOW DIET
WT VEHICLE
WT WY14643
P465L VEHICLE
P465L WY14643
HFD DIET
WT VEHICLE
WT WY14643
P465L VEHICLE
P465L WY14643
a
WT
WT WY
P465L
P465L WY
CHOW
HFD
Liver TG
T (p=0.07)
Title
2
1.5
1
0.5
0
b
HEPATIC FATTY ACID COMPOSITION (%)
MOLAR %
(p=0.07)
(p=0.06)
(p=0.1)
WT
P465L
WT-WY
P465L-WY
CHOW
HFD
SFA
PUFA
MUFA
16:00
16:01
18:00
18:1 n-9
18:1 n-7
18:2n-6
20:3 n-6
22:00
20:4 n-6
20:5 n-3
22:5 n-3
22:6 n-3
c
CHOW DIET
HFD DIET
WT
P465L
WT
P465L
VEH
WY
VEH
WY
VEH
WY
VEH
WY
4.5
6.6
9.0
dgat1
dgat2
acc1
fas
acyl
scd1
scd2
fads1
fads2
fads3
fads6
elovl1
elovl2
elovl3
elovl5
elovl6
elovl7
G
T
D
GxT
GxD
TxD
GxTxD

FIG 2

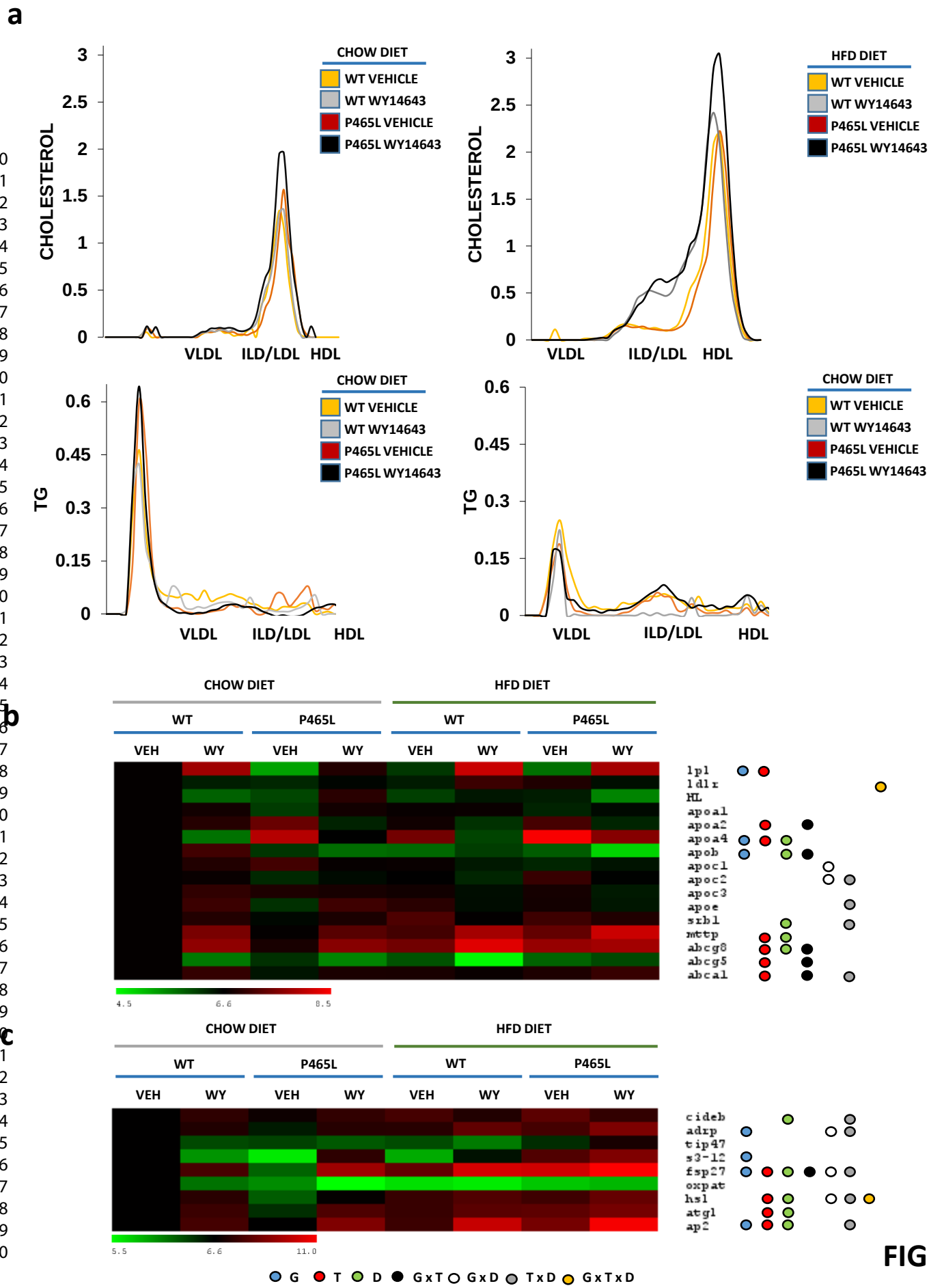
a
CHOLESTEROL
CHOW DIET
WT VEHICLE
WT WY14643
P465L VEHICLE
P465L WY14643
VLDL
ILD/LDL
HDL
HFD DIET
TG
b
WT
P465L
VEH
WY
lpl
ldlr
HL
apoa1
apoa2
apoa4
apob
apoc1
apoc2
apoc3
apoe
srb1
mttp
abcg8
abcg5
abca1
c
cideb
adrp
tip47
s3-12
fsp27
oxpat
hsl
atgl
ap2
G
T
D
GxT
GxD
TxD
GxTxD

FIG 3

a

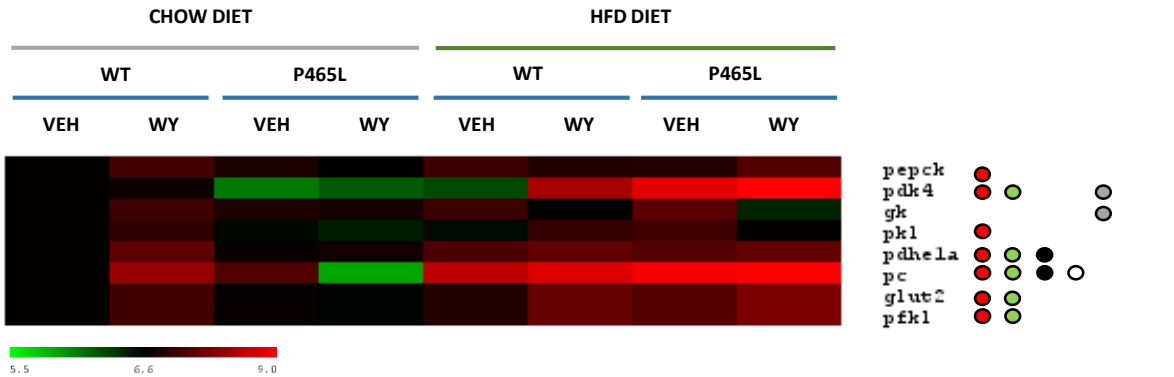
CHOW DIET
HFD DIET
WT
P465L
WT
P465L
VEH
WY
VEH
WY
VEH
WY
VEH
WY
pepck
pdk4
gk
pk1
pdhela
pc
glut2
pfk1
5.5
6.6
9.0

b

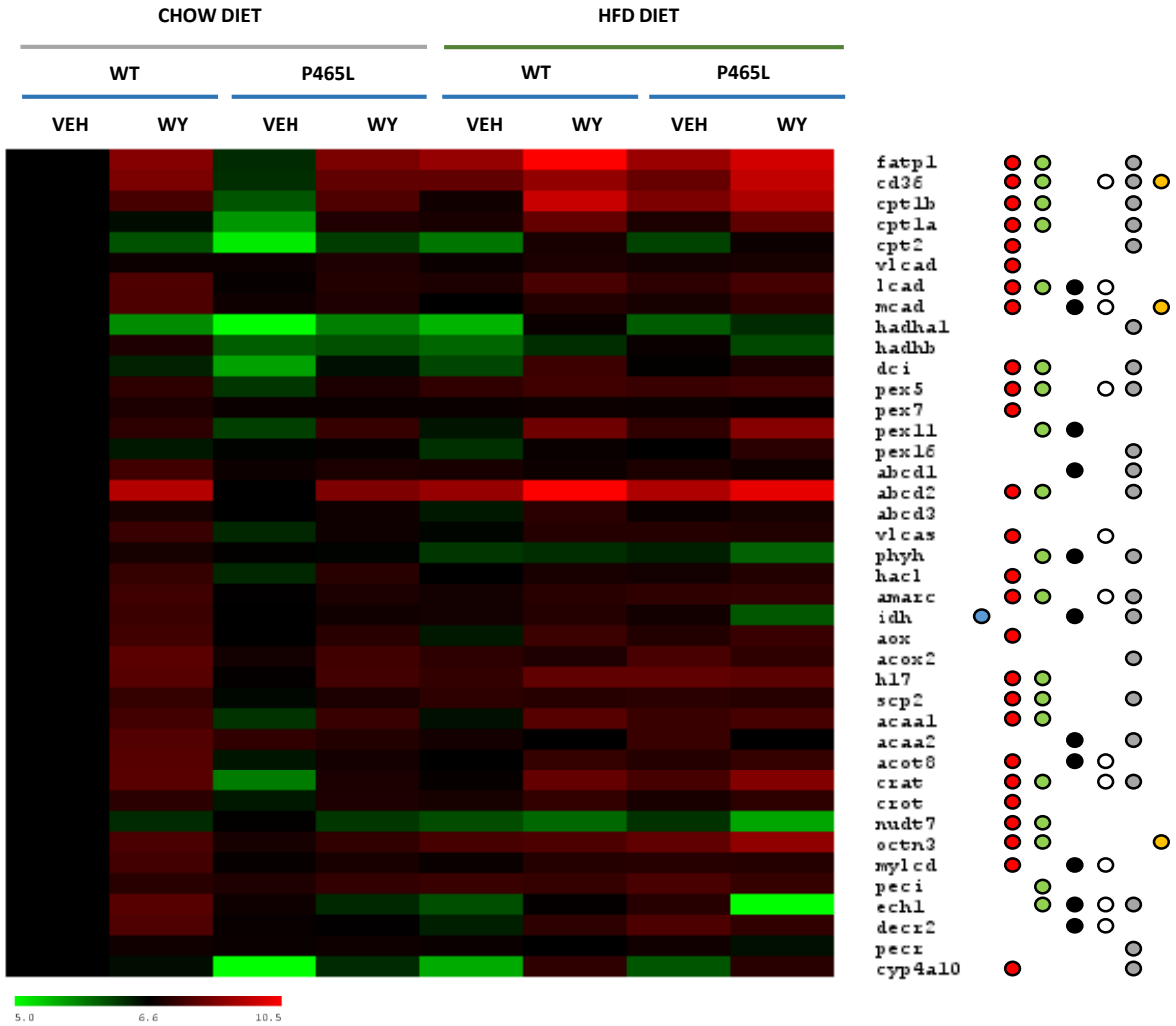
CHOW DIET
HFD DIET
WT
P465L
WT
P465L
VEH
WY
VEH
WY
VEH
WY
VEH
WY
fatp1
cd36
cpt1b
cpt1a
cpt2
vlcad
lcad
mcad
hadhal
hadhb
dci
pex5
pex7
pex11
pex16
abcd1
abcd2
abcd3
vlcas
phyh
hacl
amacr
idh
aox
acox2
hl7
scp2
acaa1
acaa2
acot8
crat
crot
nudt7
octn3
myl cd
peci
ech1
decr2
pecr
cyp4a10
5.0
6.6
10.5

c

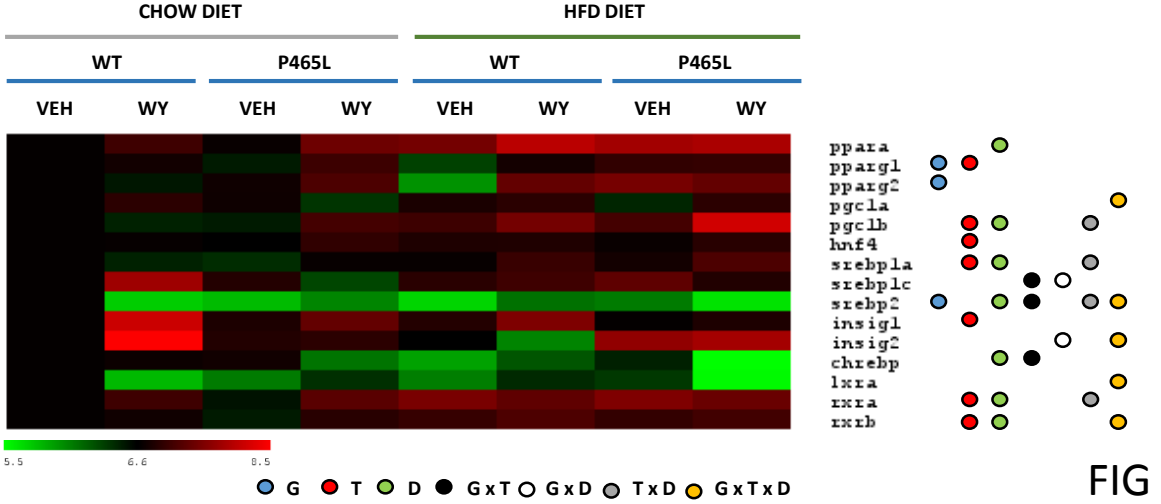
CHOW DIET
HFD DIET
WT
P465L
WT
P465L
VEH
WY
VEH
WY
VEH
WY
VEH
WY
ppara
pparg1
pparg2
pgc1a
pgc1b
hnf4
srebp1a
srebp1c
srebp2
insig1
insig2
chrebp
lxra
rxra
rxrb
5.5
6.6
8.5
G
T
D
GxT
GxD
TxD
GxTxD

FIG 4

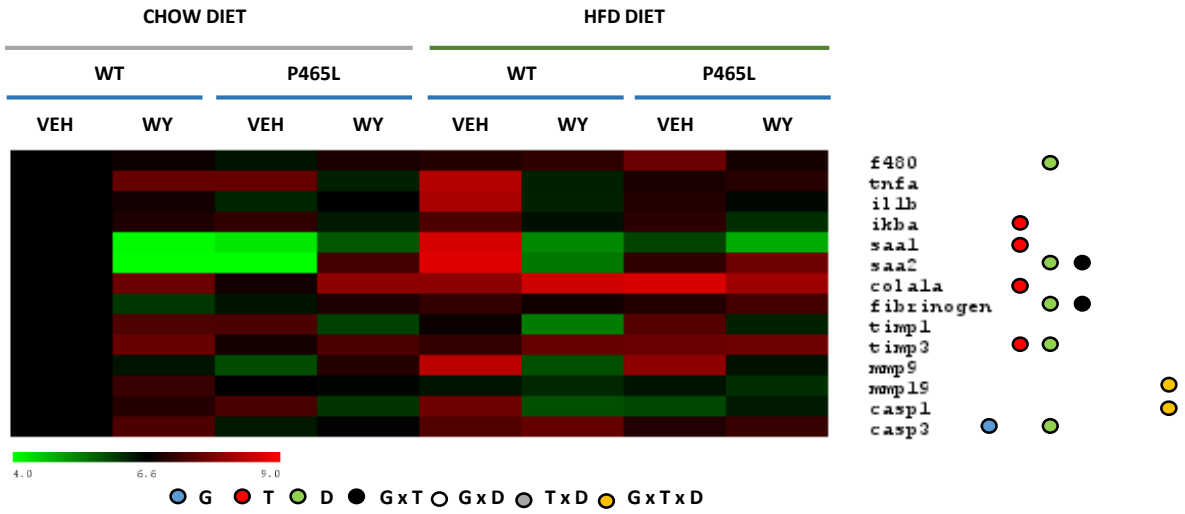
CHOW DIET
HFD DIET
WT
P465L
WT
P465L
VEH
WY
VEH
WY
VEH
WY
VEH
WY
f480
tnfa
il1b
ikba
saa1
saa2
colala
fibrinogen
timp1
timp3
mmp9
mmp19
casp1
casp3
4.0
6.6
9.0
G
T
D
GxT
GxD
TxD
GxTxD

FIG 5

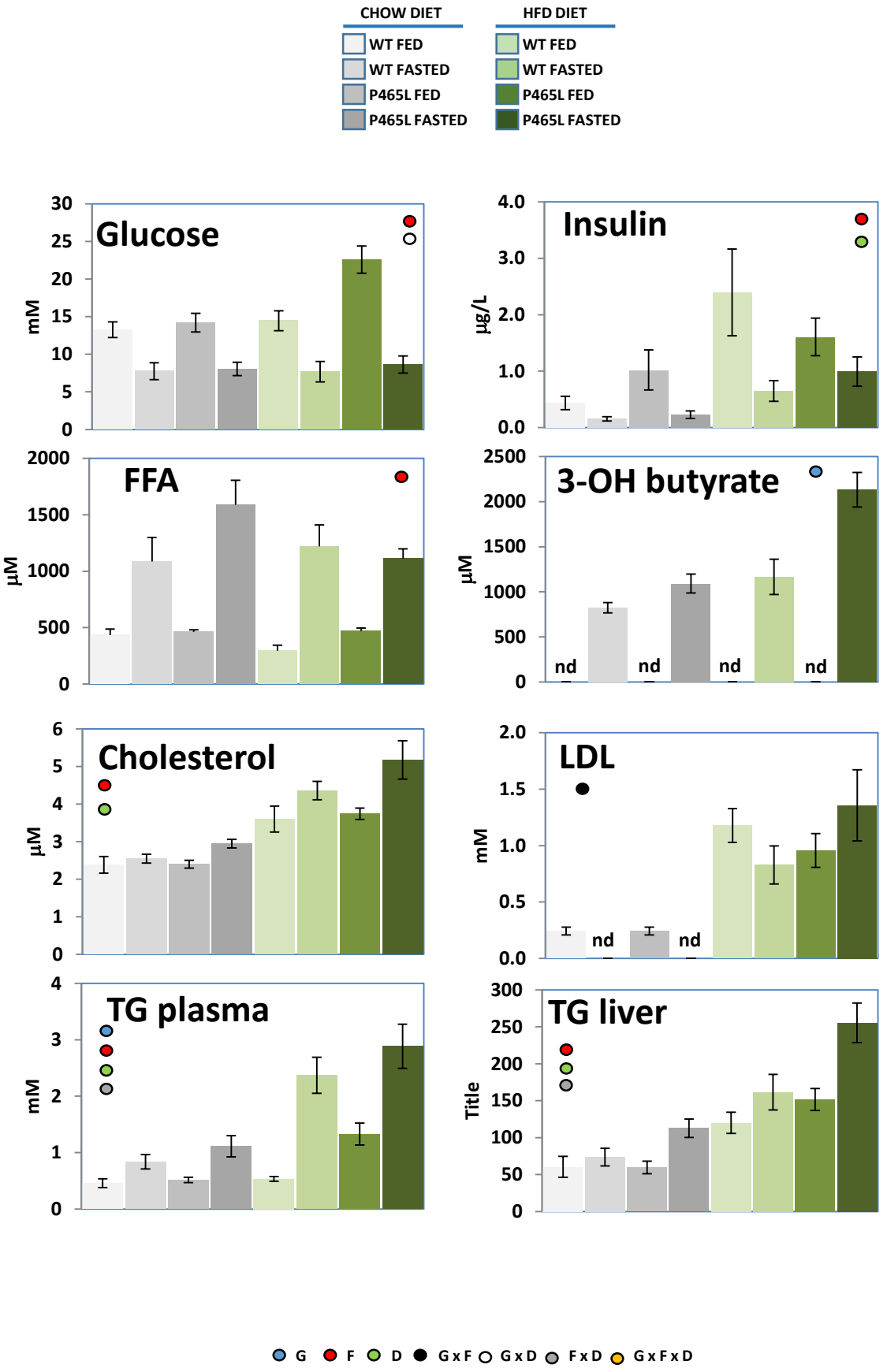
CHOW DIET
WT FED
WT FASTED
P465L FED
P465L FASTED
HFD DIET
WT FED
WT FASTED
P465L FED
P465L FASTED
Glucose
mM
Insulin
µg/L
FFA
µM
3-OH butyrate
µM
nd
Cholesterol
µM
LDL
mM
TG plasma
mM
TG liver
Title
G F D GxF GxD FxD GxFxD

SFIG 1

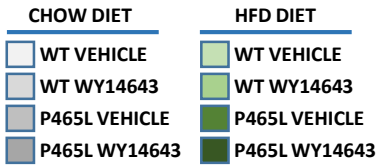
CHOW DIET
WT VEHICLE
WT WY14643
P465L VEHICLE
P465L WY14643
HFD DIET
WT VEHICLE
WT WY14643
P465L VEHICLE
P465L WY14643

a

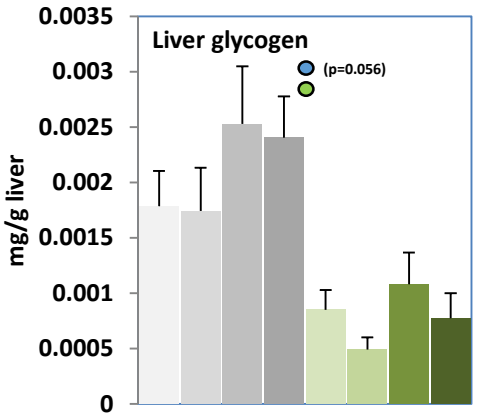
Liver glycogen
(p=0.056)
mg/g liver
0.0035
0.003
0.0025
0.002
0.0015
0.001
0.0005
0

b

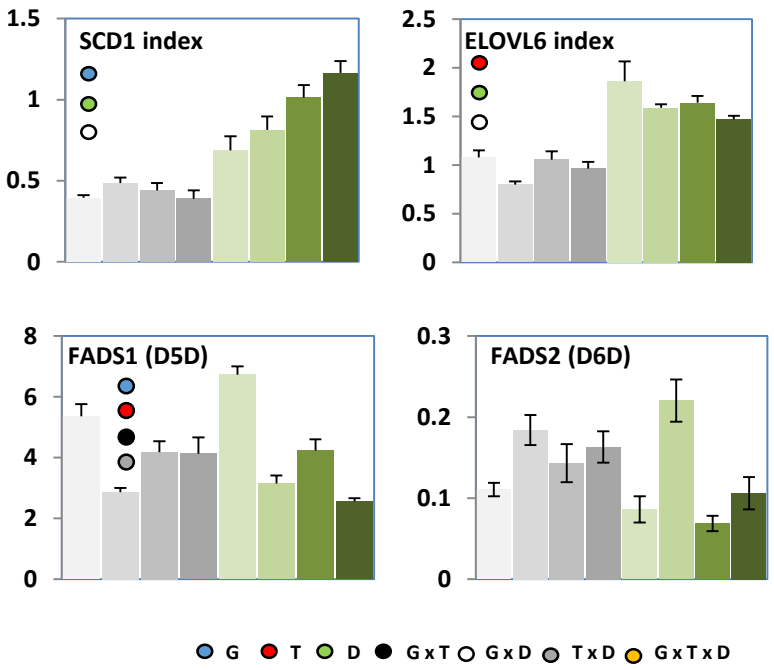
SCD1 index
ELOVL6 index
FADS1 (D5D)
FADS2 (D6D)
G
T
D
GxT
GxD
TxD
GxTxD

SFIG 2

a

Gonadal WAT

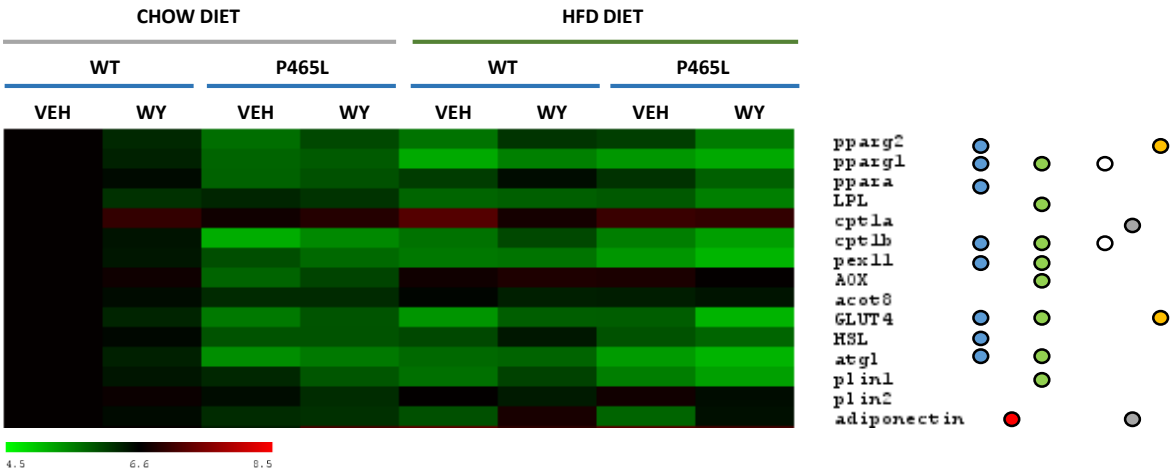

b **Skeletal Muscle**

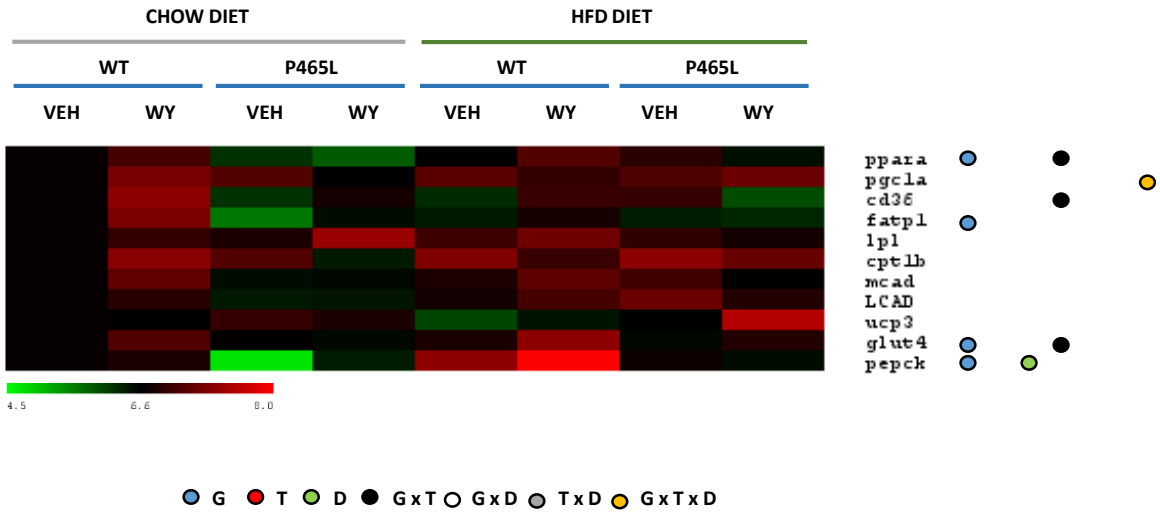

SFIG 3

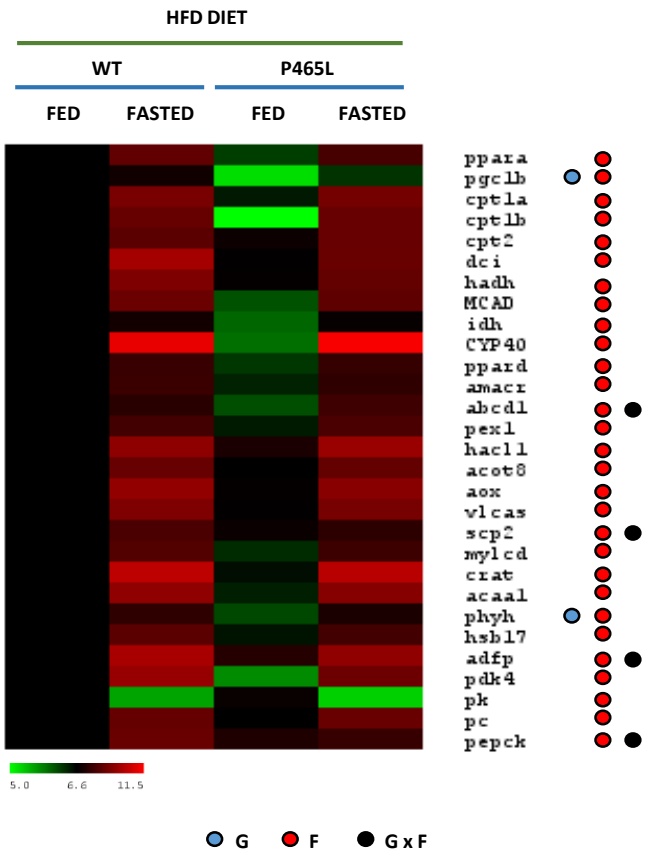
HFD DIET
WT
P465L
FED
FASTED
FED
FASTED
ppara
pgc1b
cpt1a
cpt1b
cpt2
dci
hadh
MCAD
idh
CYP40
ppard
amacr
abcd1
pex1
hacl1
acot8
aox
vlcas
scp2
mylcd
crat
acaa1
phyh
hsbl7
adfp
pdk4
pk
pc
pepck
5.0
6.6
11.5
G
F
G x F

SFIG 4

SUPPLEMENTAL FIGURE LEGENDS

SUPPLEMENTAL FIGURE 1. Blood biochemistry from P465L pparγ mutant mice vs. WT mice fed chow or HFD for 3M in the fed and fasted state. Graphs represent the average of 5-8 mice per group ± SEM analysed by ANOVA ($p<0.05$). Different colour circles denote Genotype effect (blue), fasting (red), diet (green), interactive effect genotype x fasting (black), genotype x diet (white), diet x fasting (grey) and genotype x fasting x diet (orange).

SUPPLEMENTAL FIGURE 2. (a) Hepatic glycogen levels in P465L pparγ mutant mice vs. WT mice fed chow or HFD with or without WY14643 (ip:25mg/kg). (b) Calculated SCD1, ELOVL6 and FADS1-2 ratio from data shown in Fig2b. Graphs represent the average of 5 (a) or 7-8 (b) mice per group ± SEM and analysed by ANOVA ($p<0.05$). Different colour circles denote Genotype effect (blue), treatment (red), diet (green), interactive effect genotype x treatment (black), genotype x diet (white), diet x treatment (grey) and genotype x treatment x diet (orange).

SUPPLEMENTAL FIGURE 3. (a) Gene expression in gonadal adipose tissue (a) and skeletal muscle (b) is shown as log2 conversions of average gene expression data relative to control (log2 100 = 6.6). Magnitude > 6.6 and < 6.6 denotes up- and downregulation, respectively, compared with WT, chow fed controls. (b) Hepatic levels of glycogen. Graphs represent the average of 7-8 mice per group ± SEM and analysed by ANOVA ($p<0.05$). Different colour circles denote Genotype effect (blue), treatment (red), diet (green), interactive effect genotype x treatment (black), genotype x diet (white), diet x treatment (grey) and genotype x treatment x diet (orange).

SUPPLEMENTAL FIGURE 4. (a) Expression of genes relevant for liver metabolism from P465L pparγ mutant mice vs. WT mice fed HFD for 3M in the fed and fasted state is shown as log2 conversions of average gene expression data relative to control (log2 100 = 6.6). Magnitude > 6.6 and < 6.6 denotes up- and downregulation, respectively, compared with WT, HFD fed controls. Graphs represent the average of 6-8 mice per group ± SEM and analysed by ANOVA ($p<0.05$). Different colour circles denote Genotype effect (blue), fasting (red), and interactive effect genotype x fasting (black).